RESEARCH AND ADVANCED DESIGN LABORATORY
BOX 1249, MINNEAPOLIS, MN 55440
612-853-8100

CONTROL DATA CORPORATION

CR-135405

VARIABILITY OF OZONE NEAR THE TROPOPAUSE FROM GASP DATA

By

G. D. Nastrom

Research Report No. 1
April 14, 1978
Contract NAS3-20618

For

NASA-Lewis Research Center
Cleveland, OH 44135

CONTROL DATA CORPORATION

CR-135405

VARIABILITY OF OZONE NEAR THE TROPOPAUSE FROM GASP DATA

By

G. D. Nastrom

Research Report No. 1
April 14, 1978
Contract NAS3-20618

For

NASA-Lewis Research Center
Cleveland, OH 44135

1. Report No.	2. Government Accession No.	3. Recipient's Catalog No.
NASA CR-135405		

4. Title and Subtitle	5. Report Date
VARIABILITY OF OZONE NEAR THE TROPOPAUSE FROM GASP DATA	APRIL 1978
	6. Performing Organization Code
7. Author(s)	8. Performing Organization Report No.
G. D. NASTROM	RESEARCH REPORT NO. 1
	10. Work Unit No.
9. Performing Organization Name and Address RESEARCH DIVISION CONTROL DATA CORPORATION 8100 SOUTH 34th STREET MINNEAPOLIS, MN 55440	11. Contract or Grant No. NAS3-20618
	13. Type of Report and Period Covered CONTRACTOR REPORT
12. Sponsoring Agency Name and Address NATIONAL AERONAUTICS AND SPACE ADMINISTRATION WASHINGTON, DC 20546	14. Sponsoring Agency Code

15. Supplementary Notes

PROJECT MANAGER - JAMES D. HOLDEMAN, AIRBREATHING ENGINES DIVISION, NASA LEWIS RESEARCH CENTER, CLEVELAND, OHIO 44135

16. Abstract

This report summarizes the first 22 months of ozone data from the Global Atmospheric Sampling Program. Variations in space and time are examined at nearly all scales permitted by the data. Case studies in the tropics suggest that local ozone maxima may be found in or near clouds. Preliminary seasonal mean maps of ozone during spring are presented for the Northern Hemisphere. In the troposphere over the United States during summer there is a distinct midcontinental ozone maximum. There is a diurnal variation in ozone in the upper troposphere and the daily range is about 5 ppbv. Correlations between ozone and other variables are given for the synoptic-scale and on a hemispheric scale. The possible bearing of these results on ozone transport computations is discussed.

17. Key Words (Suggested by Author(s))	18. Distribution Statement
Ozone Tropopause Variability Vertical Flux Horizontal Flux	UNCLASSIFIED - UNLIMITED

19. Security Classif. (of this report)	20. Security Classif. (of this page)	21. No. of Pages	22. Price*
UNCLASSIFIED	UNCLASSIFIED	49	

* For sale by the National Technical Information Service, Springfield, Virginia 22161

NASA-C-168 (Rev. 10-75)

TABLE OF CONTENTS

I. INTRODUCTION

This report summarizes an analysis of the first 22 months of ozone data from the Global Atmospheric Sampling Program (GASP). GASP is an ongoing effort to collect data taken with instruments placed aboard commercial B747 airliners. Details on flight routes and instrumentation are given by Holdeman, et al. (1977), and references therein. A case study of one set of typical GASP data is given by Falconer and Holdeman (1976), and some results based on the first year of GASP data are in Nastrom (1977). In some respects this report is an extension of the latter effort, but in general the analysis here has concentrated on areas not covered before, to explore new uses of the GASP data. It must be realized that each topic addressed could have been analyzed in much greater detail, often as a full study in itself. Thus, the results presented here illustrate uses of the GASP data, but certainly do not exhaust its information content.

II. DATA

A. Availability

Basic data handling procedures are described in Nastrom (1977). All ozone data used here are from the GASP measurements archived on tapes VL0001-0007 (see Holdeman, et al., 1977), which cover the period March 1975 - December 1976. A summary of the number of individual ozone observations and flights is given in Table 1. Although data are taken in all flights above 6 km altitude, the bulk of observations fall between about 10 and 12.5 km. Also, although the airliners operate over a substantial portion of the globe, some routes are flown more frequently than others. For example, Appendix A shows the seasonal distributions by location of observations made between 11 and 12 km. The boxes along the Honolulu - Los Angeles - Chicago and New York - Northern Europe routes have many more observations than most other boxes. The lack of observations over most of Asia is also clear from Appendix A. Ozone observations have been taken from airliners over the USSR (Solonin and Osetchkin, 1977), but it has not been possible to incorporate these data into the present study.

Besides the GASP data, the northern hemisphere National Meteorological Center (NMC) pressure-height and tropopause pressure fields were available at 00 and 12 GMT each day. These data were used to compute several additional parameters for each ozone observation as described in Nastrom (1977). NMC's scheme for determining tropopause pressure was changed on 17 December 1975 and, as discussed by Holdeman, et al. (1977), there appears to be a systematic difference between tropopause pressures determined from the old and new schemes. In an effort to account for these differences, 20hPa (20 mb) have been routinely subtracted from all tropopause values reported after 17 December 1975.

B. Representativeness

Besides the local (spot) ozone amount, the GASP system is designed to report the mean and standard deviation of the ozone over the last 128 seconds. As the instrument updates every 20 seconds, these statistics are thus based on seven individual readings which do not include the corresponding local value. The standard deviations are typically about 10 ppbv in the troposphere and about 20 ppbv in the stratosphere. However, standard deviations in excess of 100 ppbv are occasionally found, and a few values exceed 200 ppbv! Since such large standard deviations show that ozone can vary greatly over short horizontal distances, one could therefore question if statistics based on local ozone values are truly representative, or if an integrated ozone value would be more desirable. For various reasons, not all local values have 128s means reported with them (Table 1) and the available data base would be relatively small if only the 128s mean values were judged useful. Thus, it is of interest to compare the statistics of local ozone with 128s mean ozone values.

Table 2a compares the means and standard deviations of local ozone and 128s average ozone values for all tropospheric and stratospheric data during selected months. The means of the two data sets differ by only 1 to 11 ppbv and the standard deviations by 0 to 8 ppbv. The mean of the absolute values of the differences between individual local and 128s average values is smaller in the troposphere than stratosphere, as is the standard deviation of the differences.

In Table 2b the statistics during selected months based on all local ozone values at 30-40°N, 11-12 km, are compared with the corresponding statistics based on 128s average ozone data. In general, the correlation coefficients and other statistics given in Table 2b are nearly identical for the two data sets. Thus the local ozone values seem to be as representative as 128s averages, and throughout the remainder of this report only the analyses of local ozone values will be presented.

III. RESULTS

A. Case studies of tropical tropospheric ozone

According to the classical understanding of the ozone cycle, tropical tropospheric ozone is supplied mainly by injections from the stratosphere in mid-latitude storm systems followed by lateral transport within the troposphere. This chain of events should give rise to relatively uniform ozone amounts in the tropical upper troposphere due to mixing by Hadley cell movements, and the annual maximum in the tropics should occur a few months later than the maximum at mid-latitudes. Pruchniewicz (1973) concludes that the classical model is compatible with his aircraft and surface measurements, and suggests that injections in the mid-latitude northern hemisphere contribute the most to the tropical ozone cycle. Recently, Chatfield and Harrison (1977) studied ozonesonde data from a chain of stations extending to the Canal Zone (9°N) and conclude that the classical understanding agrees with their data. In general, the GASP data support these conclusions. Most of the flights across the equator (Table 1) show only minor variations with latitude in the tropical region, and the seasonal mean values between 15N and 15S (Appendix A) show a distinct annual maximum in September-November, in agreement with Chatfield and Harrison. However, the source of some large ozone values contributing to this seasonal maximum may not be slow transport from the northern hemisphere mid-latitudes. A few cases will illustrate this point.

Figure 1 shows the ozone mixing ratio data as a function of height and latitude from 20N - 20S for a flight from New York to Rio de Janerio and return on November 5-6, 1976. The striking features of Figure 1 are the relatively large ozone values over the equator at 179 hPa and the sharp discontinuity at 3°N. At lower levels the discontinuity is found at higher latitudes. Similar northward and downward sloping discontinuities are found on the other flights made on November 13, 21-22, and 28-29. It is noteworthy that Fabian and Pruchniewicz (1977) observed very high tropical ozone values over Africa on September 26-27 and October 2-4, 1972. They don't discuss the first case (although the large tropical values were not isolated data points as relatively large values persisted to 30°S), and state that the second case could be due to instrument failure. There is no reason to doubt the calibration of the present ozone instrument, especially in view of the apparent continuity with altitude of the observed pattern.

As values in excess of 60 ppbv are not found within 10° of the equator during any other season, these data are intriguing, and one must inquire about their origin. If these data were the result of quasi-horizontal transport from the northern hemisphere mid-latitudes the flow would have to be southward above 179 hPa and then curve back on itself near the equator to account for the positive gradient of ozone with altitude at the equator. A much more straightforward transport would be northward and downward from the springtime mid-latitudes of the southern hemisphere. However, even direct transport from the southern hemisphere doesn't seem to account for all the data. On November 21-2[illegible] (Figure 2) a secondary maximum is found near 14°N at 217 hPa. These flights were among the few which included water vapor measurements made with an aluminum oxide dew-frost point hygrometer (Holdeman, et al., 1977). Because the instrument has a slow response time (8 to 30 minutes) which varies with temperature and the gradient in dew point, the data are used here only for guidance. On November 21, saturation mixing ratio was first reported at 13.5°N. Allowing for instrument lag, the edge of the secondary ozone maximum apparently coincides with the edge of a cloud.

Further evidence for a correlation between high tropical ozone amounts and clouds was obtained on December 21, enroute from Honolulu to Pago Pago (Figure [illegible] A discontinuity in ozone occurred at about 2.5°S, the hygrometer first indicate[illegible] saturation at 5°S (about 15-20 minutes lag), and the cloud detector instrument first indicated clouds at 2.5°S. Whether the apparent correlation between clouds and high ozone is due to photochemistry, entrainment in the stratosphere, creation of ozone by lightning, or some other mechanism can't be resolved here.

The point here is that tropical tropospheric ozone has features not explained by the classical model.

B. Variations with longitude and comments on vertical transport

Variations with longitude of the total ozone are well-known from ground-based (Newell, 1964; Wilcox, et al., 1977) and satellite measurements (Ghazi, et al., 1976; Frederick, et al., 1977). Satellite data do not allow resolution of the vertical distribution of ozone below the mid-stratosphere, but the few scattered ozonesonde stations available do suggest variations with longitude in the troposphere and lower stratosphere (Dütsch, et al., 1970; Chatfield and Harrison, 1977; Belmont, et al., 1978). The ozonesonde data, however, are not adequate to support detailed studies of the geographic distribution of ozone, and it is thus of great interest to examine spatial variations as resolved by the GASP data.

The distribution with latitude and longitude of available GASP data at 11-12 km was given in Appendix A. Figure 4 shows a polar map of the mean ozone amount for spring north of 30°N. The interpolation across the USSR was guided by the data for 8-12 km given in Solonin and Osetchkin (1977). In Figure 4, there appear to be three maxima around latitude 60°N, but only two major maxima around latitude 45°N. A similar pattern is found at 10-11 km (Figure 5); the data are too few at 9-10 or 12-13 km to check for further continuity of pattern in the vertical. Presumably, the geographical distribution of ozone at these altitudes is determined primarily by variations in transport processes. However, close examination of Figures 4 and 5 and comparison with wind patterns is not warranted due to the relatively large uncertainties in these mean values as indicated by the large associated standard deviations (Appendix A). If the patterns are verified by further years of data then they will merit close attention.

Along the most heavily traveled routes, one can resolve continental-scale variations in mean ozone from the available GASP data. For example, Figure 6 shows the mean ozone amount in the upper troposphere over the United States during summer, which is typical of the other seasons. Only observations above 400 hPa and more than 20 hPa (about 0.5 km) below the tropopause were used here. The statistical data for numbered grid points in Figure 6, given in Table 3, show that the chart represents conditions near 11 km. In Figure 6, a mid-continental maximum is evident. The pattern is not caused by a few wild numbers, because it persists when only those ozone observations with less than 200, or even 100, ppbv are used (Table 3). Chatfield and Harrison (1977) have noted a similar geographical pattern at 3-7 km in annual mean ozonesonde data, but with the maximum displaced about 10° eastward, and with much smaller east-west gradients.

Following the discussion by Chatfield and Harrison, the pattern in Figure 6 may reflect the preferred regions of downward transport from the stratosphere. The westward tilt of the maximum with altitude, and the larger gradients at 11 km than at 3-7 km, seem to agree with the downward transport hypothesis. Further, the frequency distributions given in Table 3 show that observations above 100 ppbv occur most often over the central continent. It was shown in Nastrom (1977), that values greater than 100 ppbv are generally characteristic of stratospheric air. Thus, the abnormally high percentage of observations over 100 ppbv in the central continent suggest stronger flow across the tropopause there than on either seacoast, as expected from the transport hypothesis due to the mid-continental standing lee-side trough. This does not, however, imply the mechanism by which the trans-tropopause flow occurs. One might suggest "stratospheric injections" in the tropopause folds of developing baroclinic systems (cf., Danielsen, 1968), but cyclogenesis is uncommon over the central United States in summer (Hovanec and Horn, 1975). On the other hand, there could be creation or downward transport of ozone in the mid-continental thunderstorms. Finally, the largest ozone values are found over Illinois and Missouri, coincident with a trough in the mean flow at 200 hPa, suggesting that ozone may be transported across the tropopause by the vertical motions of large-scale wave systems. The latter mechanism is consistent both with the present results and with the results of Chatfield and Harrison.

C. Variations with latitude and time

The variation of ozone at 217 hPa (11.3 km in the standard atmosphere) is given in Figure 7 as a function of latitude and month. Pressure has been used here as the vertical coordinate to allow direct comparison between the northern and southern hemispheres. The annual cycle of ozone is easily seen almost to the equator in the northern hemisphere, a small semiannual oscillation is seen near the equator in the second year, but there is insufficient data to detect any cycles in the southern hemisphere. Although the present data are limited, it is interesting to consider possible systematic differences between the hemispheres.

In order to perform a more objective inter-hemispheric comparison, hemispheric differences were computed for corresponding seasons. The data were combined at each latitude and altitude into four 3-month seasons (March, April, May was spring). The hemispheric differences (Figure 8) are large and negative poleward of 30° during summer and winter, indicating larger values in the southern hemisphere, while a reversed pattern is found during spring. Equatorward of about 20° the differences are small with no definite pattern during winter, but the southern hemisphere values are consistently larger during spring and summer and smaller during autumn.

These results agree well with Pittock's (1977) comparison of ozonesonde data at 200 mb at Aspendale (38^{o}S) and Boulder (40^{o}N), and are particularly significant since the period of record and longitudinal coverage of the present data is much different. There is no southern hemisphere ozonesonde station other than Aspendale which has a large number of soundings, so the large gradient in hemispheric differences near 35^{o}-40^{o} latitude can be confirmed only by further GASP measurements.

Returning to Figure 7, the pattern of contours presents a different image from year-to-year, especially during late spring at mid-latitudes. A very simple method to objectively analyze the interannual differences as functions of height and latitude is to compare the location of a typical contour during corresponding months of the two years. This is done in Figure 9 where the 100 ppbv contours for selected months have been traced from analyzed height-latitude sections. Clearly the month-to-month variations within a year are far greater than any interannual variations. This agrees with the results of Wilcox, et al. (1977), who found that near the tropopause the amplitude of the annual wave is about an order of magnitude greater than that of the quasi-biennial oscillation.

In an effort to quantify the amplitudes and phases of the time-periodic waves in the data in Figure 7, an analysis was made using the multiple-regression technique reported in Belmont and Dartt (1973). Frequencies included in the analysis were the long-term mean and the first three harmonics of the annual wave. As only the annual wave's results had relatively small statistica errors and a definite pattern of phase progression, only they are reproduced in Figure 10. A sharp horizontal gradient of amplitude is found near the southern most location of the mean tropopause, and a uniform phase progression persists into the subtropics. The maximum of the annual wave occurs in late spring in the mid-latitude lower stratosphere, and in early summer at 15^{o}N, the lowest latitude with reliable phase data shown in Figure 10. This phase progression pattern agrees well with that of Wilcox, et al. (1977), but differs from the latitude-seasonal perspectives at 5-7 km given by Chatfield and Harrison (1977) which show the subtropical maximum in August or September. This difference, however, is probably due to higher altitude of the present data and the much more vigorous horizontal transport processes in the upper troposphere compared to the mid-troposphere. By June the southward leg of the Hadley cell is established above about 9 km from 15^{o}N to 30^{o}S (Newell, et al., 1972). Further, the transport by eddy motions in the low-latitude upper-troposphere is much stronger than that in the lower troposphere (Newell, et al., 1969). Thus, the periodic analysis results given here agree with past work, and can generally be explained by the classical model of the ozone cycle.

D. Diurnal variation of ozone in the upper troposphere

Diurnal variations in lower tropospheric ozone have been studied by several writers, but little work has been reported on ozone above the planetary boundary layer. There is some hint of a systematic variation in ozone between dawn and mid-day in the sonde data at one station presented by Chatfield and Harrison (1976), but extending their analysis is hampered by the tendency for most sonde stations to schedule observations at the same time each day. The GASP data offer a unique opportunity to examine diurnal ozone variations in the upper troposphere because they are taken at all hours of the day and over a wide range of latitudes.

Before the diurnal variations can be studied it is necessary to remove, as well as possible, variations due to all other causes. In an effort to account for spatial variations, the data were stratified into vertical layers 20 hPa deep starting 10 hPa below the tropopause, and into latitude bands 16° wide. For each layer/latitude, annual and interannual variations were accounte for by subtracting the mean over all data in each season from the individual tri-hourly means during the same season. These seasonal tri-hourly means were then averaged (weighting each by the number of observations) to obtain the fina tri-hourly means, which were then smoothed with a 1-2-1 filter.

Examples of the waveforms of these data are given in Figure 11. Although the confidence limits are relatively broad, the waveform is very similar for both levels in each latitude band, and data at the two northernmost latitude bands are remarkably similar. Even though the data shown have been smoothed, some irregularities remain. These could be real, but are most likely due to sampling differences between seasons for a given hour because at some latitudes a smoother waveform results when the seasonal means are averaged without regard for each season's number of observations (Figure 12). Note also that the general shape of the seasonal waves in Figure 12 is the same for all seasons.

The waveforms in Figure 11 are too regular to attribute to chance, but they could arise from sampling bias just as well as from a real diurnal variation. For example, if all nighttime observations were made at the north end of a latitude band and all daytime observations at the south end, then the normal variation of ozone with latitude would induce an apparent diurnal wave. Howeve close examination of the distribution of data with latitude and longitude does not reveal any systematic bias. For example, Table 4 shows the frequency distribution of observations at 30-50 hPa below the tropopause from 32-48°N. There is no obvious pattern in the distributions in Table 4 which could be used to explain the waveform in Figure 11, nor could a pattern be found at other levels or latitudes. Therefore, the waveforms are believed to represent a genuine diurnal variation in ozone in the upper troposphere.

The amplitudes and phases (time of maximum) of the diurnal waves are given in Table 5. These were analyzed using the periodic regression techniques of Belmont and Dartt (1973). In general, the amplitudes range from 1-6 ppbv at all locations. The phases are in late morning at most levels at 32°-64°N, but are in late evening at 16-32°N. There is no obvious physical explanation for this phase discontinuity, but several alternative mechanisms could be presented to explain the presence of any diurnal ozone variation. For one, tropospheric photochemistry is expected to produce a diurnal variation in ozone (e.g., Chameides and Walker, 1976). The photochemistry could be based on the mean observed water vapor, or it could include a diurnal variation in water vapor to account for the observed diurnal variation in precipitation and cloud parameters (Wallace, 1975). Alternatively, the diurnal variation in convection (perhaps associated with precipitation) might also cause upward mixing of the ozone-depleted boundary layer, or entrainment in clouds penetrating the tropopause might result in increased downward transport of ozone from the stratosphere, or some other mechanism may be involved. As pointed out by Chatfield and Harrison (1977), there is no easy way to support or to reject many of these possible mechanisms.

E. Correlation relationships of ozone with other variables

1. Synoptic-scale

It has long been recognized that the amount of ozone at a given location is strongly influenced by changes in the atmospheric circulation. In Nastrom (1977), the east-west variation in ozone was found to have an autocorrelation function which resembles a damped cosine with wavelength near 2150 km, based on 33 carefully selected flight segments. This feature has now been verified using 111 flight segments, selected on the same criteria as before. The expanded data set has also been used to study the mean synoptic scale relationships between ozone and temperature and wind as discussed next.

Figure 13 shows the distance-lagged cross-correlation functions for ozone and temperature and wind speeds. Data points are nominally spaced five minutes i.e., 75 km, apart. Only flight segments over 1500 km long and primarily east-west were used here. Also, the data were sorted so that the westernmost observations on each flight always came first in the analysis routines. In the stratosphere, ozone and temperature are well-correlated at lag zero, but the correlation falls off rapidly with distance. The distance between successive minima in the autocorrelation function is 2250 km, nearly the same as the characteristic wavelength found for ozone variations. Ozone and meridional wind are poorly correlated at lag zero, but ozone amounts correlate well with the meridional wind speeds 600 km to the east. Twice the distance between the maximum and minimum correlation coefficients is about 2400 km, only slightly longer than the characteristic wavelength of ozone. In the tropospher the correlation between ozone and meridional wind speed is nearly the same as i the stratosphere. The correlation between tropospheric ozone and temperature, however, is poor. The correlation between ozone and zonal wind speed closely resembles that for meridional wind speed, except the phase is shifted by about a quarter-wavelength so the most negative correlation occurs at lag zero.

The phase lag relationships discussed above were quantified by the method of cross-spectral analysis, and the results are given in Table 6 for the frequency band centered at wavelength 2250 km. As it is estimated there are about 40 degrees of freedom for the stratospheric data and 20 for the tropospheric data, coherency squared values greater than 0.27 and 0.38, respectively, are significant at the 5% level. Note that all phases tend to be nearly integer multiples of 90°, with largest deviations from this occurring for small coherency squared. Together with the geostrophic approximation, these phase lag relations show that ozone and pressure-height are out of phase in synoptic scale systems near the tropopause (Figure 14). This relation may be useful for approximating the synoptic-scale ozone distribution from conventional meteorological data because on a given pressure-height map largest ozone will be found with lowest height.

The small correlations at lag zero between ozone and meridional wind in Figure 13 illustrate the difficulty in obtaining reliable estimates of the meridional ozone flux. One form of the flux equation is

$$\text{Flux} = \sigma_1 \sigma_2 \mathcal{r}_{12}$$

where subscripts identify variables 1 and 2. As standard deviations (σ) are always positive, the sign of the flux is determined by the sign of the correlation coefficient ($\mathcal{r}$). Thus, the present data indicate northward meridional ozone flux in the lower stratosphere and southward flux in the troposphere, in agreement with the results given in Nastrom (1977). However, many observations are required to ensure confidence in even the sign of flux estimates. For example, about 375 independent pairs of data are required to give 95% confiden that a measured correlation coefficient of +0.05 is not from a population whose true value is -0.05. This underscores the relatively large uncertainty in all flux computations, especially when a small data sample is used.

2. Large-scale

In those regions and over those time periods when ozone can be considered chemically inert and the air motion adiabatic, ozone and potential vorticity are both conserved following the flow. As both of these parameters have a stratospheric source and a sink near the ground, they are generally well correlated. Other parameters, such as temperature, are also correlated with ozone although not as well as potential vorticity because the dynamic coupling is not as intimate. The correlations between ozone and dynamic variables is a matter of practical, as well as theoretical, intrinsic interest. For example, Pruchniewicz (1973) used the correlation of ozone with scalar wind speed in a model to study stratospheric-tropospheric exchange, Danielsen and Mohnen (1977 used potential vorticity to estimate the downward flux of ozone at the tropopause, and Belmont, et al. (1978), used temperature to crudely estimate ambien ozone levels in the lower stratosphere. Each of these efforts was partly stim lated by the relative abundance of routine meteorological data compared to ozo data, and for this reason future writers will likely continue to use the corre lation between ozone and other parameters. It is thus worthwhile to examine the effects of smoothing, or averaging, on the correlations with ozone.

It was shown in Nastrom (1977) that in the lower stratosphere ozone correlates about equally well with temperature and potential vorticity.

However, the data used did not have the same spatial resolution. The temperature and ozone data were local observations taken on the aircraft, while the potential vorticity data were computed from the highly smoothed NMC pressure-height fields. Presumably, the correlation coefficients for potential vorticity would be higher if they were derived from fine-scale data, as ozone and temperature are. It is not possible to test this with the present data, but the inverse problem (smoothing the ozone data) can be studied. Table 7 shows the correlation coefficients between ozone and potential vorticity for all available Northern Hemisphere data by month. In the first row, the coefficients were computed with no smoothing or averaging applied, but in the second row the individual observations were averaged over 1 km in height and 10° in latitude to form monthly mean grid-point values in the meridional plane, which were then used to compute the correlation coefficient. A grid-point value was disregarded if it was based on fewer than 20 individual observations. During all months, averaging the data to form grid points improves the correlation between ozone and potential vorticity.

IV. SUMMARY AND CONCLUSIONS

The GASP observations are relatively plentiful, widely distributed in space and time, and have simultaneous measurements of routine meteorological parameters, ozone, and (occasionally) other trace species. The GASP data have been found to be adequate to support several new studies not previously possible, and to expand on some past studies which were made using conventional ozone data. The following conclusions have been reached:

1. Local ozone measurements yield the same large-scale statistics as 128-second average ozone measurements.

2. The GASP data are now sufficiently numerous to crudely resolve longitudinal and latitudinal differences in mean ozone amounts, and to permit interhemispheric comparisons at several latitudes. These first results are tentative and must be verified by further data. In particular, an effort must be made to obtain compatible data over the Soviet Union. This recommendation was made in Nastrom (1977), and by Solonen and Osetchkin (1977).

3. Some features of the tropical ozone distribution are not easily explained by the classical transport theory, and there is evidence of higher ozone levels in tropical clouds.

4. Continental-scale variations of ozone in the upper troposphere seem associated with standing waves in the height field. This suggests that the vertical ozone flux at the tropopause is associated with large-scale motion systems as tacitly assumed by Nastrom (1977).

5. There is a diurnal variation in ozone in the upper troposphere. The daily range is about 5 ppbv.

6. Synoptic-scale zonal ozone variations show a predominant wavelength near 2150 km. For this wavelength, ozone is in phase with temperature, out of phase with zonal wind, and nearly in phase quadrature with meridional wind. It will thus require many independent pairs of wind and ozone observations to determine the algebraic sign of the meridional flux with confidence.

7. When the fields of ozone and potential vorticity are smoothed by space-time averaging, the correlation between them is improved.

REFERENCES

Belmont, A. D. and D. G. Dartt, 1973: Semiannual variation in zonal wind from 20 to 65 kilometers at $80^{o}N-10^{o}S$. J. Geophys. Res., 78, 6373-6376.

Belmont, A. D., R. W. Wilcox, G. D. Nastrom, D. N. Hovland, and D. G. Dartt, 1978: Guidelines for flight planning during periods of high ozone occurrence. Report No. FAA-EQ-78-03, 161pp.

Chameides, W. and J. Walker, 1976: A time-dependent photochemical model for ozone near the ground. J. Geophys. Res., 81, 413-420.

Chatfield, R. and H. Harrison, 1976: Ozone in the remote troposphere: Mixing versus photochemistry. J. Geophys. Res., 81, 421-423.

Chatfield, R. and H. Harrison, 1977: Tropospheric ozone 2. Variations along a meridional band. J. Geophys. Res., 82, 5969-5976.

Danielsen, E. F. and V. A. Mohnen, 1977: Project Dustorm Report: Ozone transport, in situ measurements, and meteorological analyses of tropopause folding. J. Geophys. Res., 82, 5867-5877.

Danielsen, E. F., 1968: Stratospheric-tropospheric exchange based on radioactivity, ozone, and potential vorticity. J. Atmos. Sci., 25, 502-518.

Dutsch, H., W. Zullig, and Ch. Ling, 1970: Regular ozone observations at Thalwil, Switzerland and Boulder, Colorado. LAPETH-1, Zurich, 279pp.

Fabian, P. and P. G. Pruchniewicz, 1977: Meridional distribution of ozone in the troposphere and its seasonal variations. J. Geophys. Res., 82, 2063-2073.

Falconer, P. and J. Holdeman, 1976: Measurements of atmospheric ozone made from a GASP-equipped 747 airliner: mid-March, 1976. Geophys. Res. Lett. 3, 101-104.

Frederick, J. E., B. W. Guenther, and D. F. Heath, 1977: Spatial variations in tropical ozone: The influence of meridional transport and planetary waves in the stratosphere. Beitr. Phys. Atm., 50, 596-507.

Ghazi, A., A. Ebel, and D. F. Heath, 1976: A study of satellite observations of ozone and stratospheric temperature during 1970-1971. J. Geophys. Res., 81, 5365-5373.

Holdeman, J. D., D. J. Gauntner, F. M. Humenik, and D. Briehl, 1977: NASA Global Atmospheric Sampling Program (GASP) data report for tapes VL0007 and VL0008. NASA TM-73784, 56pp.

Hovanec, R. D. and L. H. Horn, 1975: Static stability and the 300 mb isotach field in the Colorado cyclogenetic area. Mon. Wea. Rev., 103, 628-638.

REFERENCES (Cont'd)

Nastrom, G. D., 1977: Variability and transport of ozone at the tropopause from the first year of GASP data. NASA-CR-135176, 28pp.

Newell, R. E., 1964: Further ozone transport calculations and the spring maximum in ozone amount. Pure Appl. Geophys., 59, 191-206.

Newell, R. E., D. G. Vincent, and J. W. Kidson, 1969: Interhemispheric mass exchange from meteorological and trace substance measurements. Tellus, 5, 641-647.

Newell, R. E., J. W. Kidson, D. G. Vincent, and G. J. Boer, 1972: The General Circulation of the Tropical Atmosphere, MIT Press, Chapter 3.

Pittock, A. B., 1977: Climatology of the vertical distribution of ozone over Aspendale (38^{o}S, 145^{o}E), Quart. J. R. Met. Soc., 103, 575-584.

Pruchniewicz, P. G., 1973: The average tropospheric ozone content and its variation with season and latitude as a result of the global ozone circulation. Pure Appl. Geophys., 106-108, 1058-1073.

Solonin, S. V. and V. V. Osetchkin, 1977: Aircraft investigations of atmospheric ozone concentration over the USSR. Preprint distributed at the IAGA/IAMAP Assembly, Seattle, August 22 - September 3, 12pp.

Wallace, J. M., 1975: Diurnal variations in precipitation and thunderstorm frequency over the conterminous United States. Mon. Wea. Rev., 103, 406-419.

TABLE 1. Summary of GASP ozone data.

Month	Total Observations	Total Flights	128-second Means	Equator Crossings
1975 Mar	1263	57		
Apr	554	26		
May	1625	66		6
Jun	908	35	606	
Jul	78	3		
Aug	434	16		
Sep	579	23	533	
Oct	716	25	660	
Nov	0			
Dec	326	10	281	
1976 Jan	1119	36	1022	
Feb	1435	54	1308	2
Mar	1636	59	948	
Apr	3872	126		6
May	1252	62		
Jun	225	4		
Jul	1043	35		2
Aug	4086	129		27
Sep	3272	79		2
Oct	1075	25	1031	
Nov	3247	58	2684	9
Dec	2804	86	2639	15

TABLE 2(a). Comparative statistics of the 128 second average ozone values (0-128) and of the corresponding local ozone values. Data are taken from all latitudes. T = Troposphere, S = Stratosphere. Units are ppbv.

Month	T or S	N	Local		0 128		Local minus 0-128			
			Mean	St. Dev.	Mean	St. Dev.	Mean abs. Value	Max	Min	St. Dev.
Jun 1975	T	570	97	93	96	93	10	110	-147	17
	S	36	381	157	370	149	29	162	-43	43
Sep 1975	T	514	55	41	53	40	5	57	-55	9
	S	19	184	85	188	83	13	47	-45	19
Dec 1975	T	202	41	20	39	21	5	51	-26	8
	S	79	175	78	172	75	12	119	-43	21
Mar 1976	T	528	80	58	81	58	6	51	-102	11
	S	420	358	195	357	195	22	127	-214	36
Oct 1976	T	180	79	44	81	46	8	35	-140	17
	S	851	257	125	258	124	17	149	-152	28
Dec 1976	T	1732	64	53	63	53	5	85	-242	11
	S	907	215	163	214	163	14	195	-216	28

TABLE 2(b). Comparison of statistics of 128-second average ozone values with statistics of all spot ozone values at 30-40°N, 11-12km. Units are ppbv. DELP is the tropopause separation pressure ($P_{Trop} - P_{Aircraft}$).

Month		N	Mean	St. Dev.	Correlation Coefficients: DELP	Potential Vorticity	Temp	Spot Ozone	Meridional eddy flux ($x\,10^{-8}$ g cm^{-2} s^{-1})
Jun 1975	128 s	151	102	82	.32	.55	-.10	.97	-1.1
	Spot	191	108	87	.36	.60	-.05	--	-0.5
Sep 1975	128 s	150	53	31	.15	.67	.16	.98	0.7
	Spot	156	54	30	.15	.66	.15	--	0.7
Dec 1975	128 s	79	58	61	.68	.47	.39	.98	0.2
	Spot	89	57	59	.62	.50	.39	--	0.2
Mar 1976	128 s	76	239	138	.81	.69	.78	.98	4.9
	Spot	133	229	174	.76	.71	.77	--	3.8
Nov 1976	128 s	250	83	74	.79	.83	.58	.99	0.0
	Spot	277	81	71	.80	.84	.64	--	0.5
Dec 1976	128 s	260	107	70	.80	.76	.51	.98	0.4
	Spot	264	109	72	.81	.76	.53	--	0.3

TABLE 3. Selected grid point data in the troposphere in summer. The grid point numbers refer to the locations given in Figure 6. The two right hand columns are the mean ozone at each grid point disregarding values in excess of 200 ppbv and 100 ppbv, respectively.

Gridpoint Identification						Percent of obs. by amount						Means of data	
Number	Lat (N)	Long (W)	N	Median Altitude (km)	Mean Ozone	<50	<100	<150	<200	<250	≥250	<200	<100
1	30-34	120-132	82	11.4	62 ppbv	58%	34	2	2	2	2	50 ppbv	47
2	34-38	120-132	245	11.3	63	38	52	9	0	0	1	61	55
3	34-38	108-120	104	11.2	89	29	42	18	5	1	5	75	57
4	38-42	96-108	99	11.6	81	26	48	18	3	4	0	75	62
5	38-42	84- 96	69	11.1	97	36	39	12	6	1	7	70	54
6	38-42	72- 84	28	10.7	72	46	46	0	0	0	8	52	52
7	42-46	60- 72	72	11.4	72	12	72	15	0	0	0	72	65

TABLE 4. Percentage frequency distribution of observations taken at 32-48°N between 30 and 50 hPa below the tropopause as a function of (a) longitude, and (b) latitude, for tri-hourly times of the day.

	Local Time	1-4	4-7	7-10	10-13	13-16	16-19	19-22	22-1
	N	33	61	49	254	215	103	181	76
(a)	0- 60°W	3%	11	22	5	2	6	3	0
	60-120°W	15	10	0	4	6	0	1	13
	120-180°W	22	18	39	60	47	44	26	24
	180-120°E	45	61	39	30	34	31	43	42
	120- 60°E	15	0	0	1	11	19	28	21
	60- 0°E	0	0	0	0	0	0	0	0
(b)	44- 48°N	33	11	6	19	15	3	14	29
	40- 44°N	0	15	27	26	24	46	19	17
	36- 40°N	12	15	18	35	31	19	35	24
	32- 36°N	55	59	49	20	31	32	33	30

TABLE 5. Amplitude (ppbv) and phase (hour of maximum, local time) of the diurnal wave in tropospheric ozone. Statistical error estimates, in ppbv and hours, are given in parentheses. Note the abrupt phase change at 32°N.

Distance below Tropopause (hPa)	10-30	30-50	50-70	70-90	90-110
48-64°N	1.8(.3) 1130(.5)	1.7(.3) 1000(.7)	2.7(.5) 0915(.7)	0.7(0.7) 1930(5.0)	(No data)
32-48°N	2.3(.3) 0100(.5)	2.1(.3) 0815(.5)	1.3(.3) 0730(.9)	1.3 (.3) 0700(1.0)	3.6 (.4) 1310(1.0)
16-32°N	2.3(.3) 1700(.6)	2.7(.3) 1600(.5)	5.8(.7) 1900(.5)	0.6(0.1) 2100(1.0)	5.1(.7) 1800(.6)

TABLE 6. Relative phase lags among ozone, temperature, and wind for the spectral band centered at 2250 km wavelength. Positive phase means the parameter on the top leads the parameter along the side. The coherency-squared is given in parentheses and is underlined if it exceeds the 95% confidence limit. Data are from all seasons and latitudes, but are stratified by (a) stratosphere (60 flights), and (b) troposphere (27 flights).

		Temperature	Meridional Wind	Zonal Wind
(a)	Stratosphere			
	Ozone	2°(.<u>35</u>)	86°(.17)	168°(.10)
	Temperature	---	88 (.<u>43</u>)	172 (.15)
	Meridional Wind	---	---	94 (.23)
(b)	Troposphere			
	Ozone	-121(.01)	94(.<u>39</u>)	178(.07)
	Temperature	---	79(.05)	-35(.10)
	Meridional Wind	---	---	87(.04)

TABLE 7. Linear correlation coefficients between ozone and potential vorticity, for all Northern Hemisphere data. Grid-point data are averaged over 1 km in height and over 10° in latitude.

	1975										1976											
	M	A	M	J	J	A	S	O	N	D	J	F	M	A	M	J	J	A	S	O	N	D
Individual Pairs	.78	.73	.73	.65	-	.56	.68	.72	-	.78	.83	.72	.73	.71	.73	.70	.70	.63	.80	.73	.78	.71
Grid Points	.97	.94	.97	.90	-	.98	.85	.97	-	.99	.91	.94	.92	.96	.95	.96	.92	.86	.95	.86	.96	.88

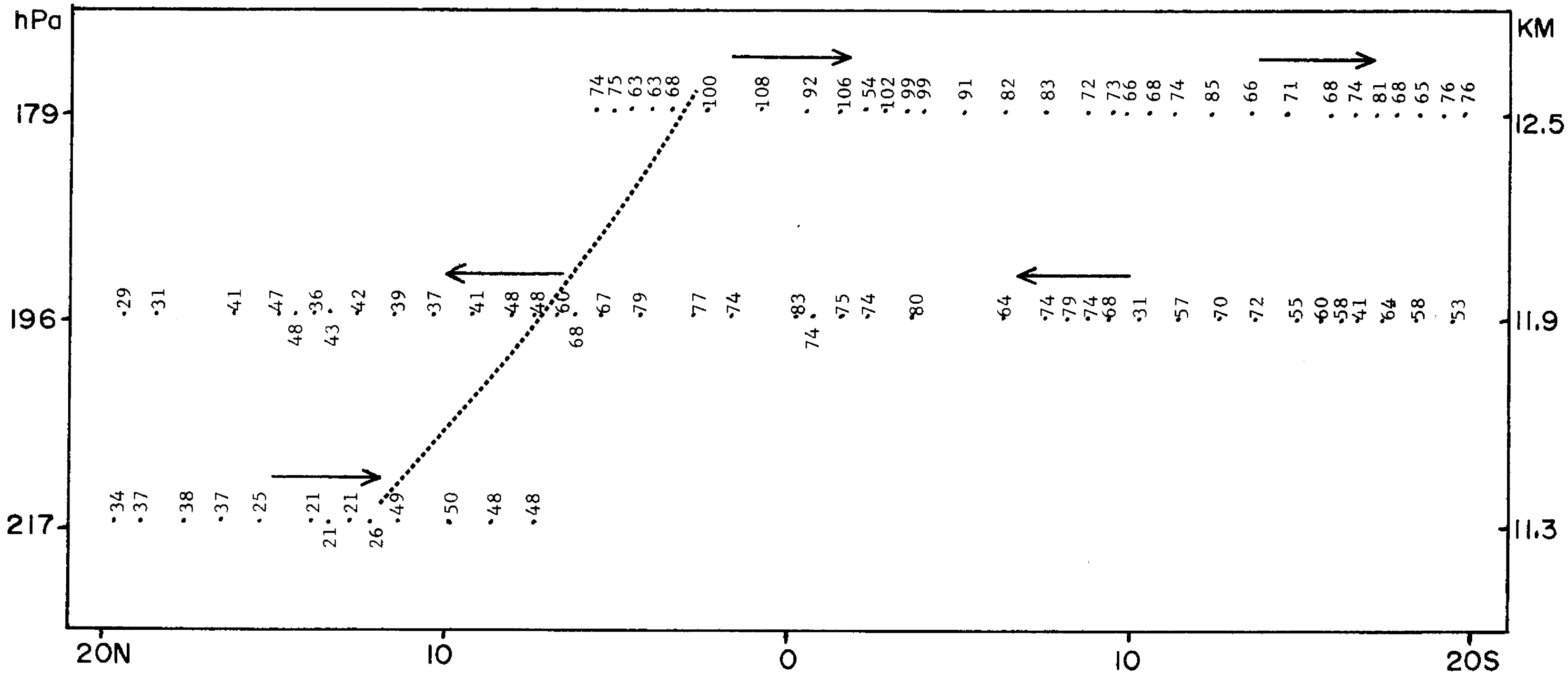

Figure 1. Ozone data (ppbv) along a flight from New York to Rio de Janerio and return on November 5-6, 1976. Arrows show direction of travel at each pressure level; the dotted line shows the ozone discontinuity. The aircraft crossed the equator at 56W southbound, and at 53W northbound. Standard atmosphere altitudes corresponding to each flight level pressure are indicated on the right.

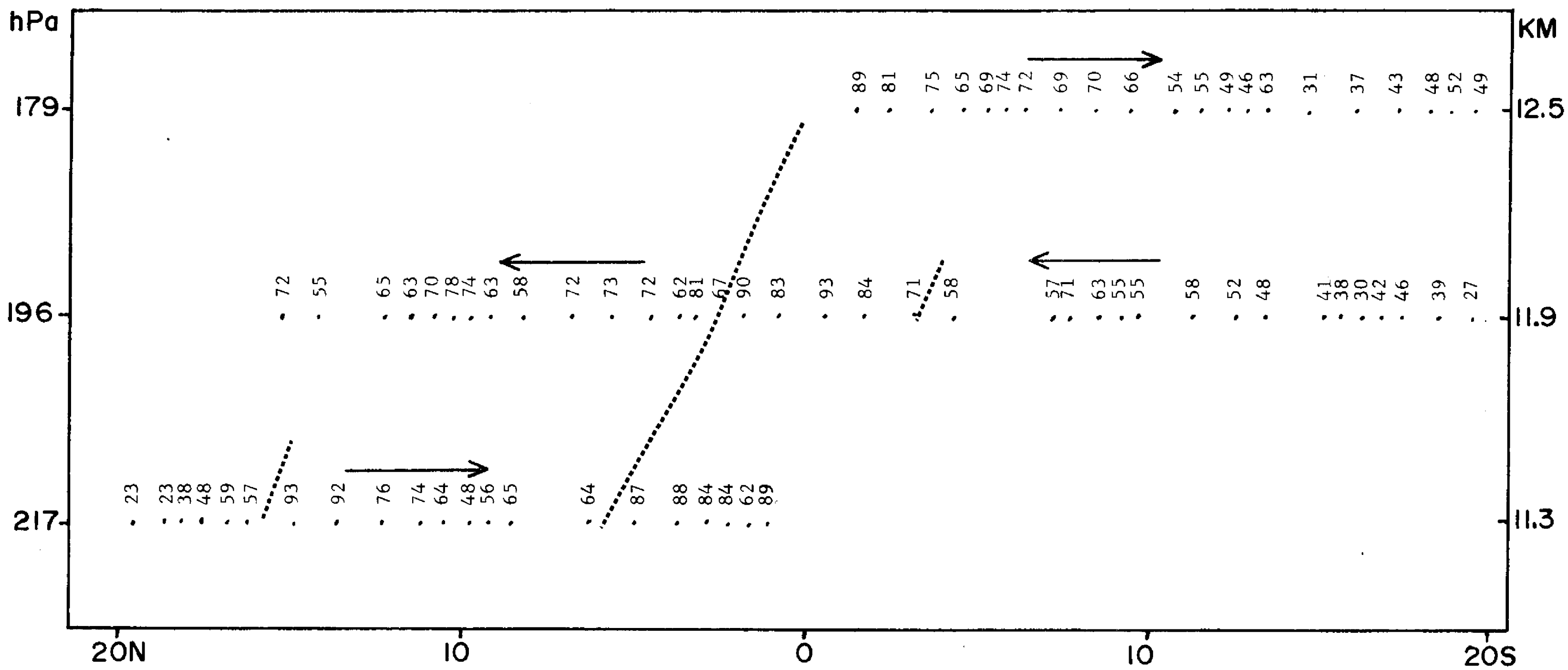

Figure 2. As in Figure 1 for November 21-22, 1976. The aircraft crossed the equator at 53W on both of these flights.

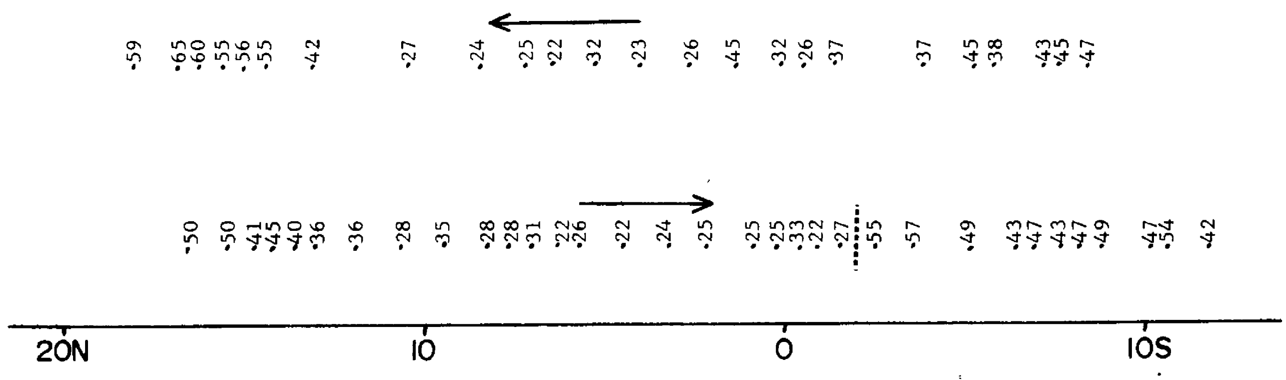

Figure 3. Ozone data (ppbv) along a flight from Honolulu to Pago Pago and return on December 21-22, 1976. Both flights were made at 179 hPa (about 12.5 km in the standard atmosphere), and both crossed the equator at 165W. The ozone discontinuity near 2S on the southbound flight coincides with a jump in moisture and with a response by the cloud detector.

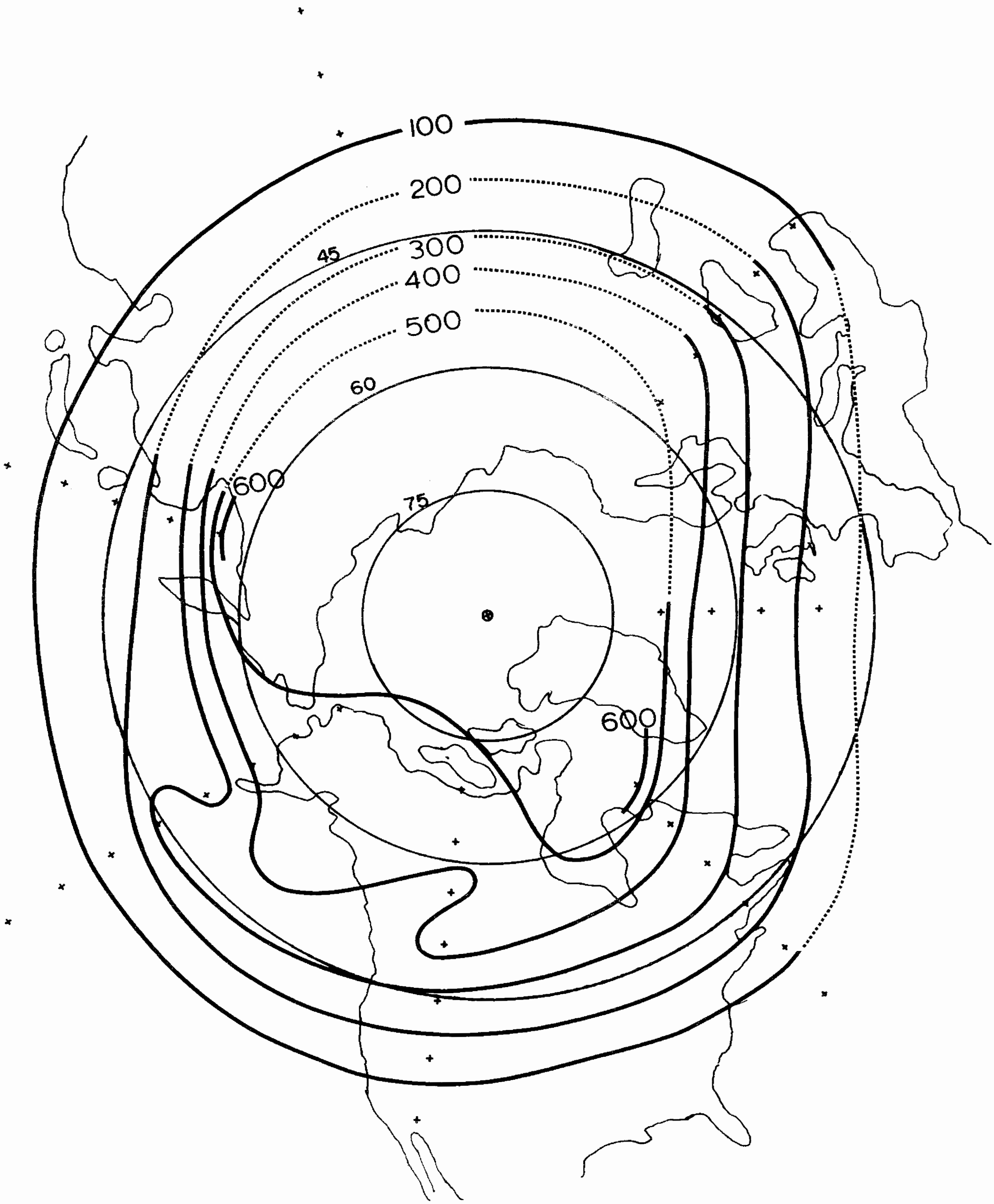

Figure 4. Mean ozone (ppbv) at 11-12 km during March - May from data given in Appendix A. Grid boxes which have data are centered on small crosses. Circles of latitude at 45, 60 and 75N are given. See text.

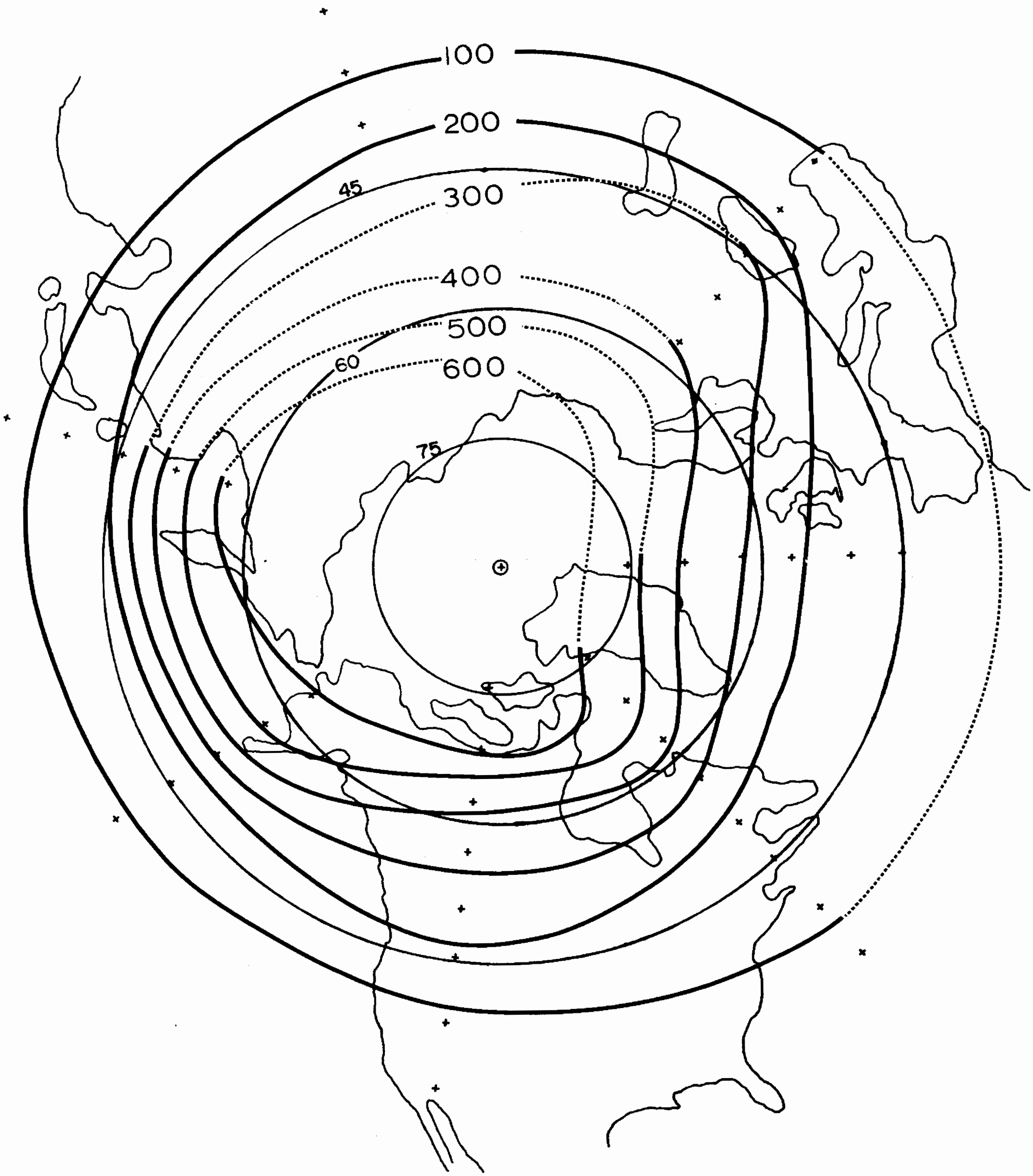

Figure 5. Mean ozone amount (ppbv) at 10-11 km during March-May. Grid boxes which have data are centered on small crosses. Circles of latitude at 45, 60, 75N are given.

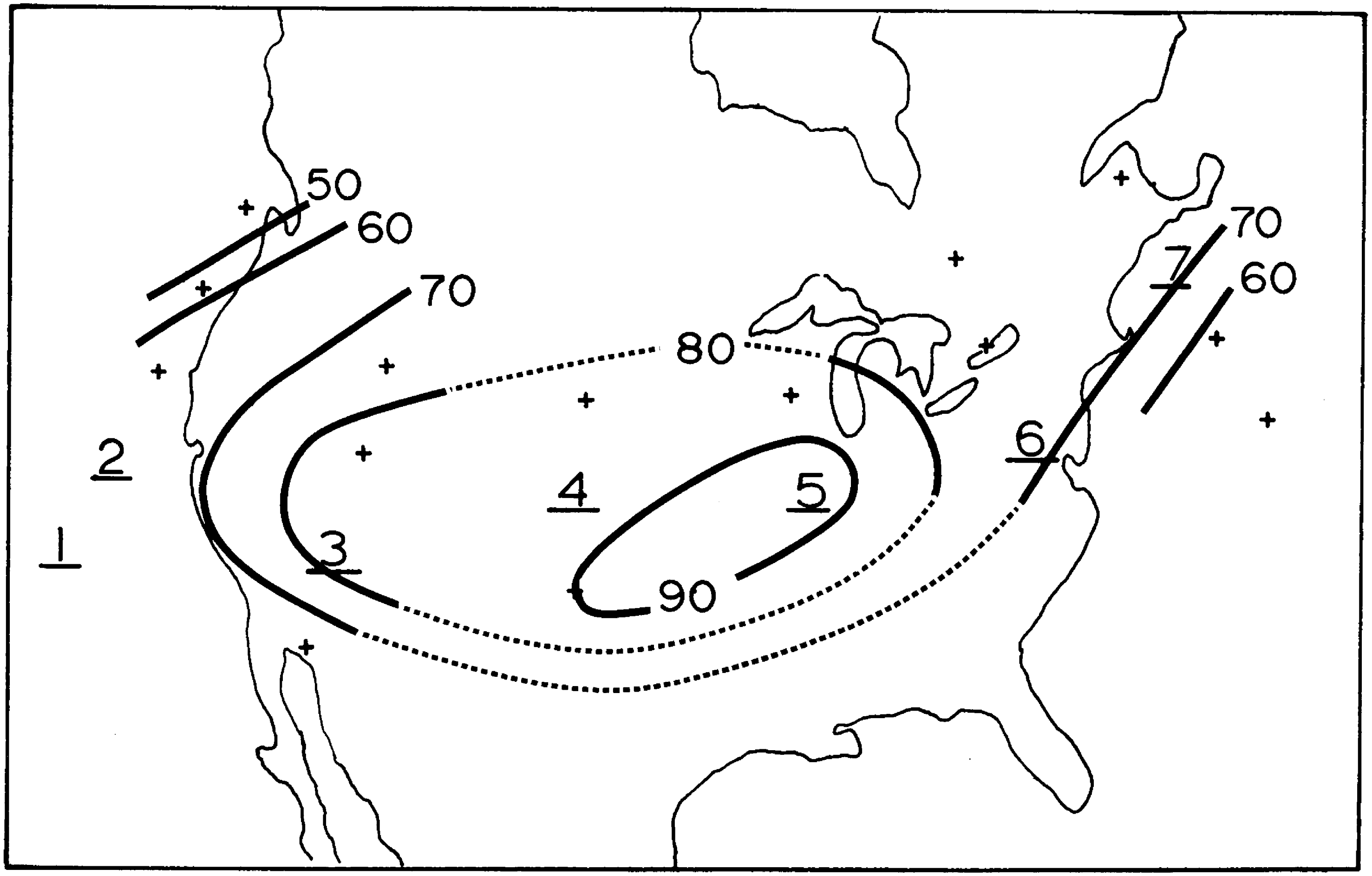

Figure 6. Mean ozone amount (ppbv) above the 400 hPa level but at least 20 hPa below the NMC tropopause during June-August. Grid points which have data are centered on small crosses, except that the seven grid points given in Table 3 are shown here by underlined numbers.

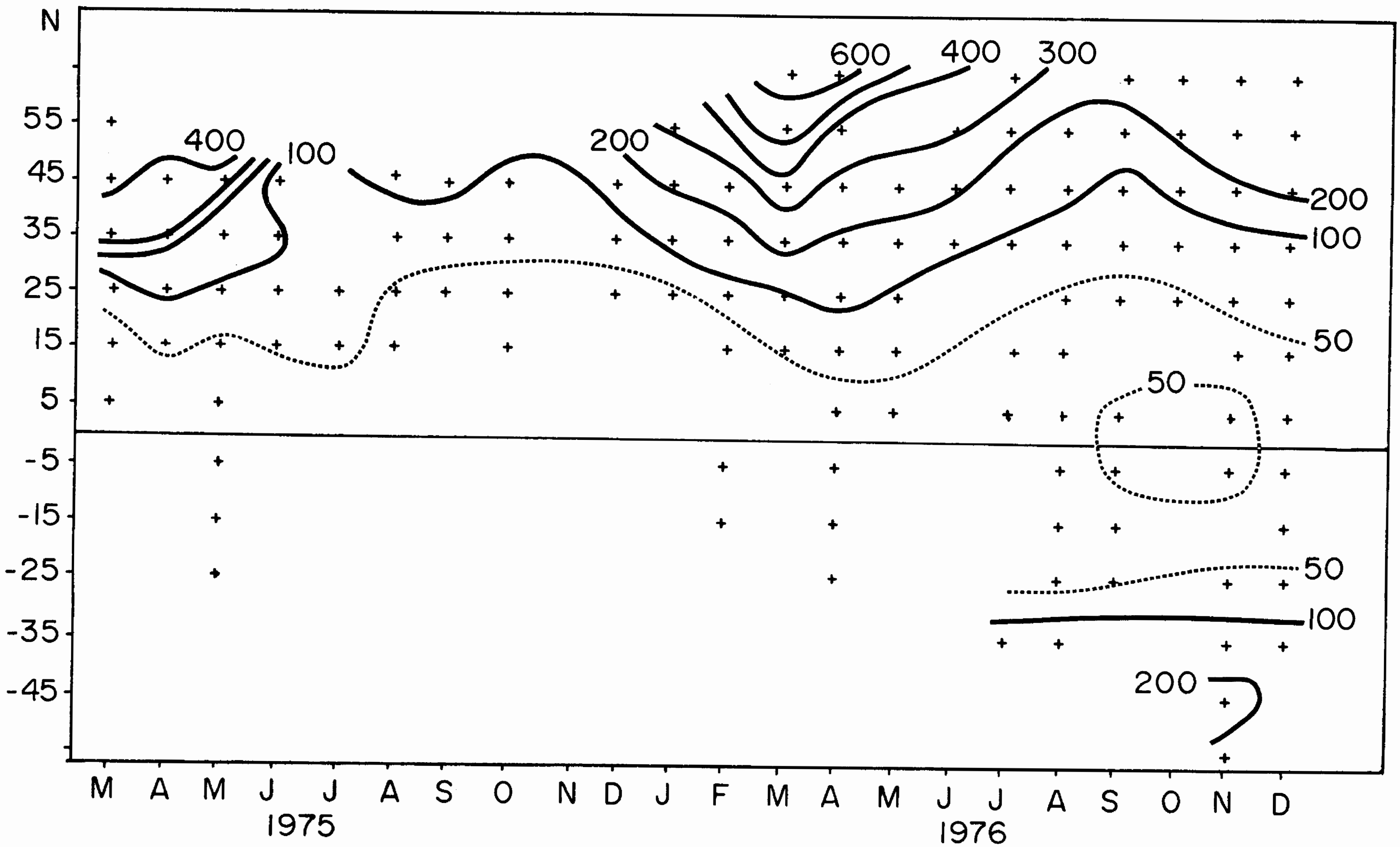

Figure 7. Zonal-monthly mean ozone amount (ppbv) for data taken at 217 hPa (37000 $\pm$ 1000 feet in the standard atmosphere, or about 11.3 km). Those grid points with data are depicted by small crosses.

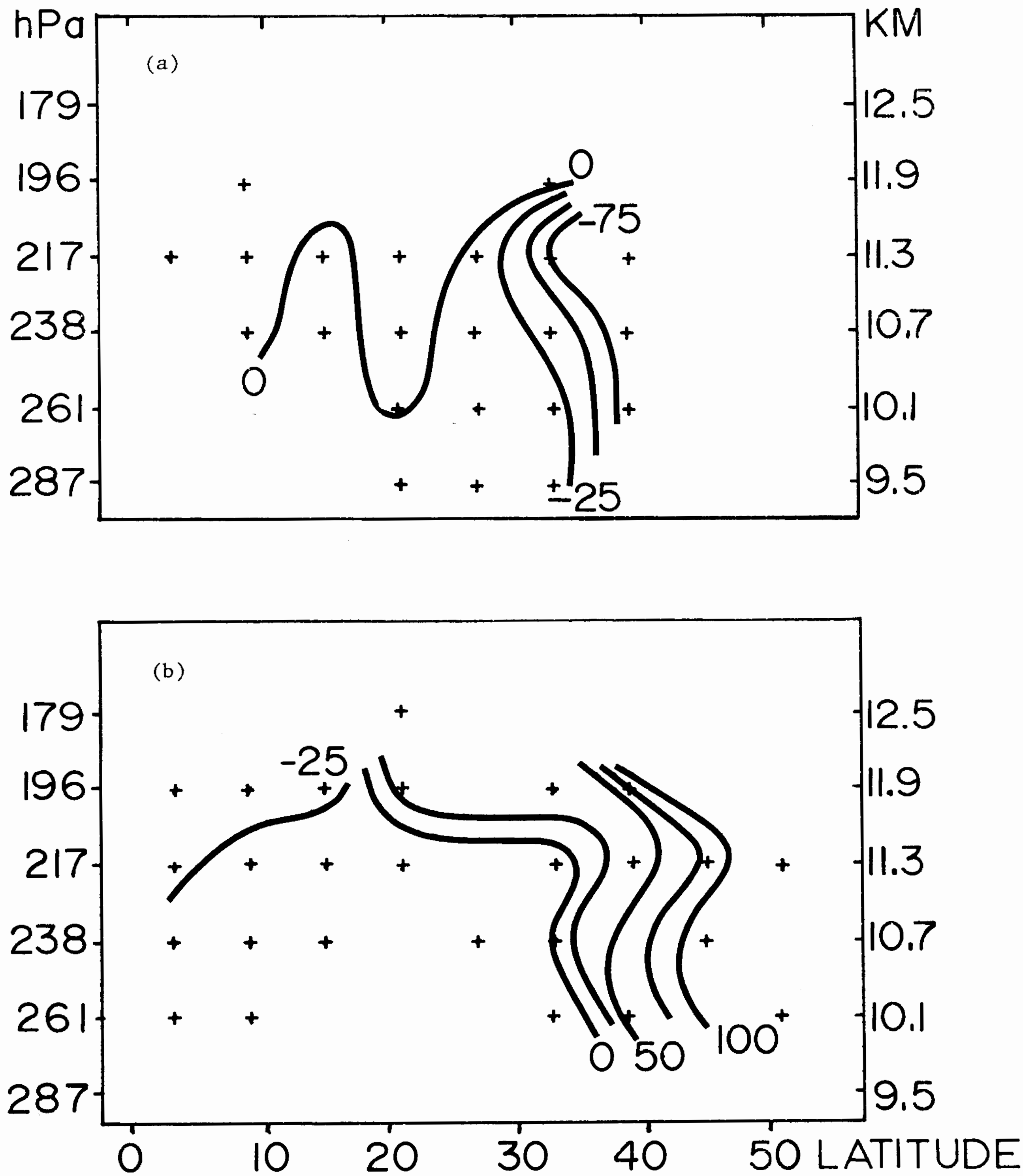

Figure 8. Northern hemisphere minus southern hemisphere seasonal zonal mean ozone amounts (ppbv) as a function of latitude and pressure. Note that 6^{o} latitude bands are used. Small crosses depict grid points with data in both hemispheres.

(a) NH winter - SH winter

(b) NH spring - SH spring

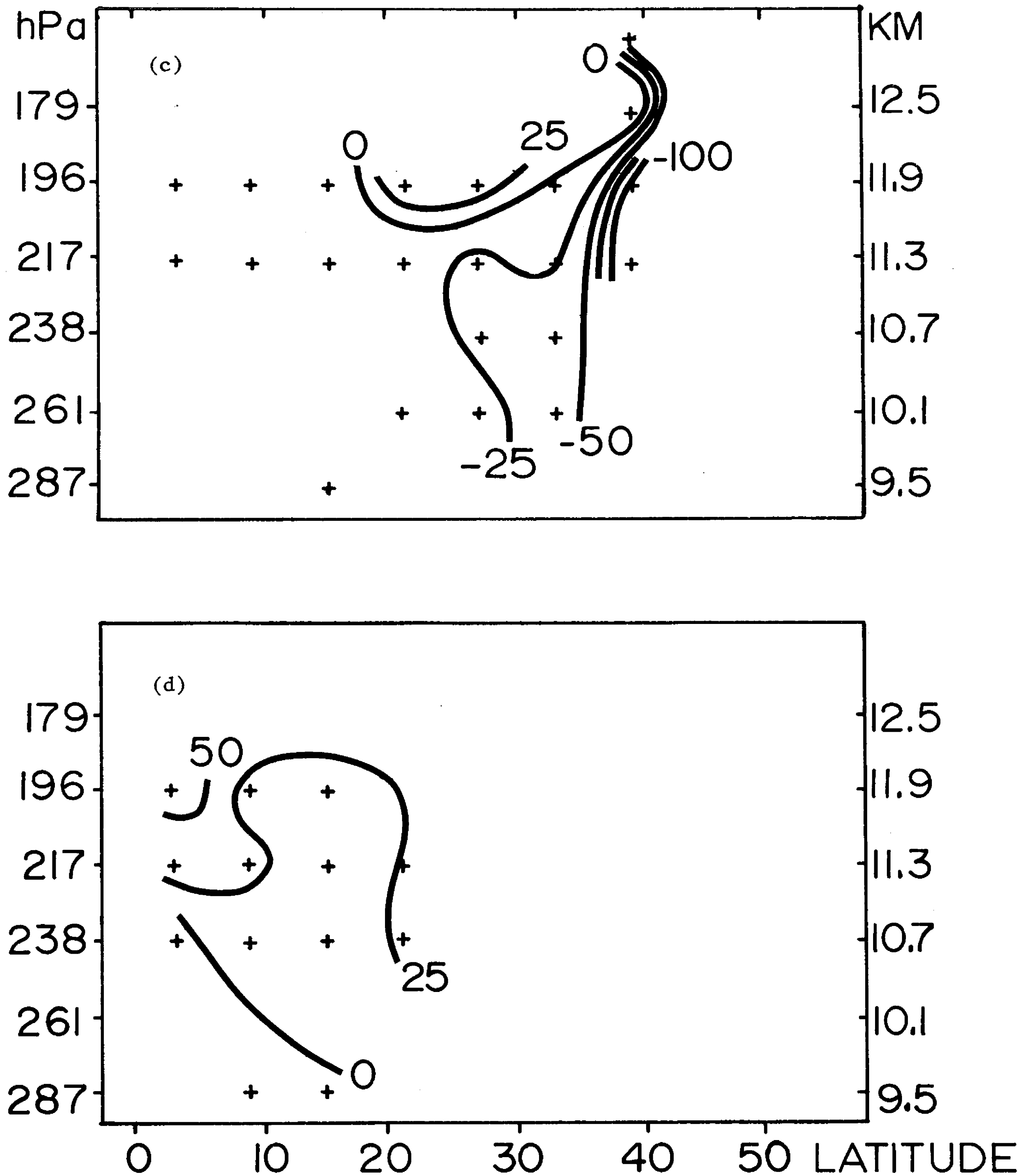

Figure 8. Continued

(c) NH summer - SH summer

(d) NH autumn - SH autumn

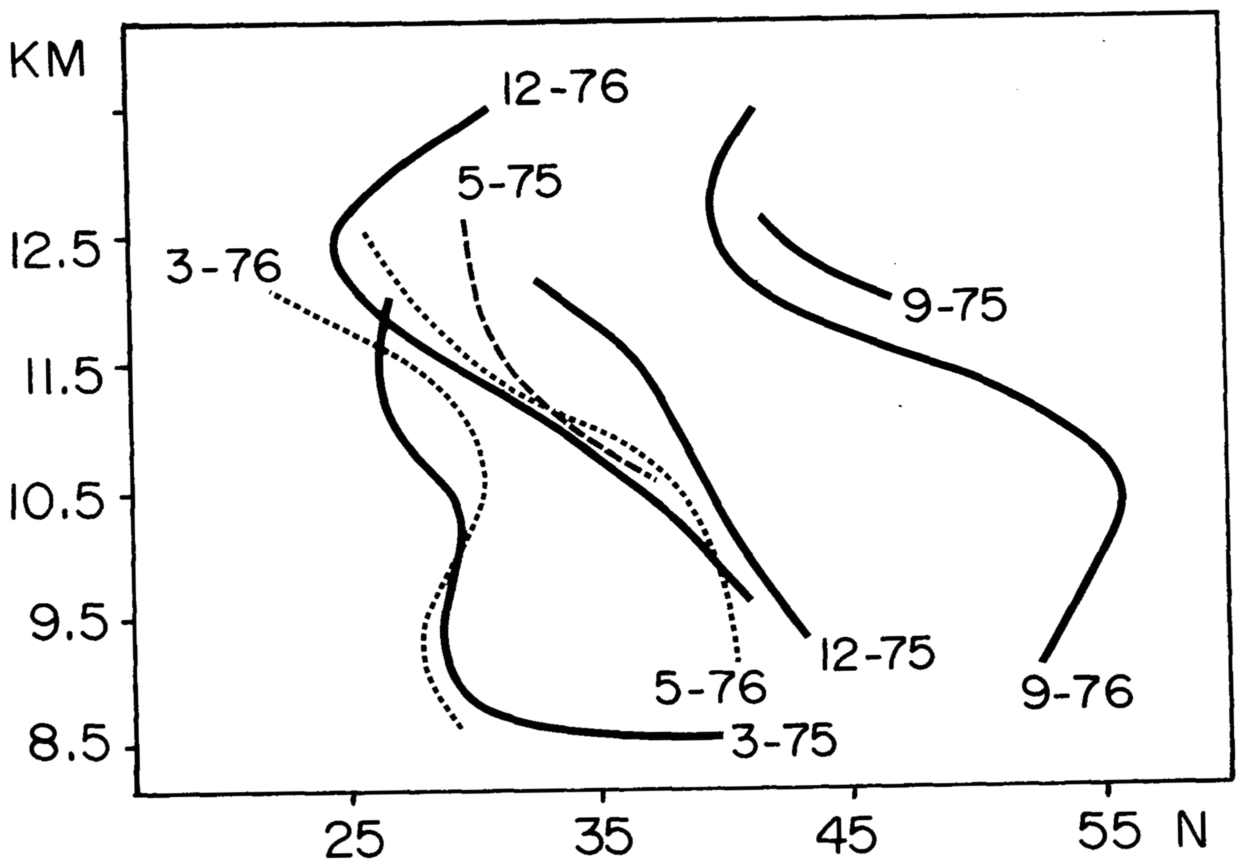

Figure 9. Location of the 100 ppbv contour as a function of height and latitude for March, May, September, and December of 1975 and 1976. Note that the variation within a year is much greater than the variation between years.

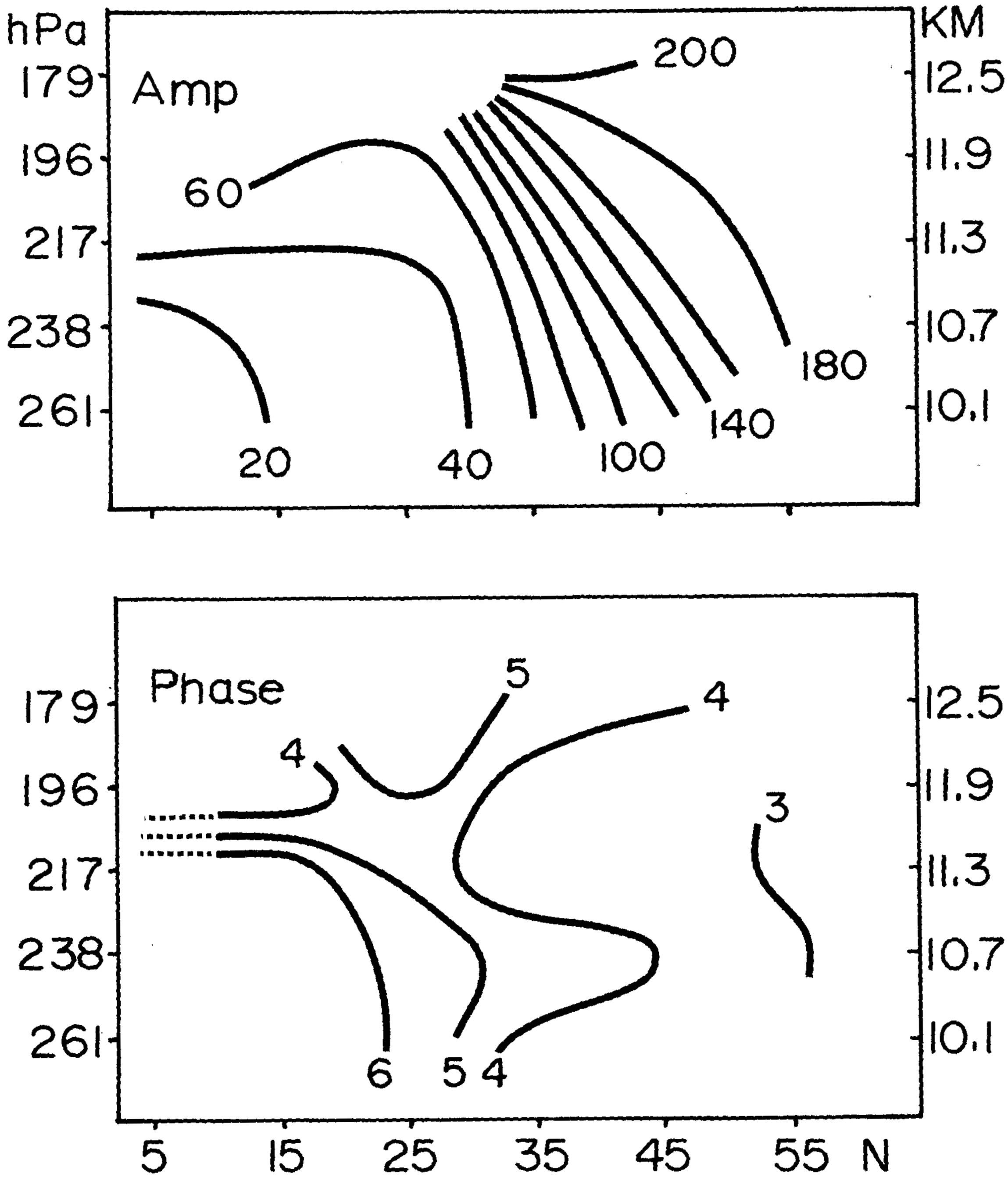

Figure 10. Periodic analysis results for the annual wave. Upper: amplitude in ppbv, lower: phase (date of maximum), contours refer to first day of the month indicated.

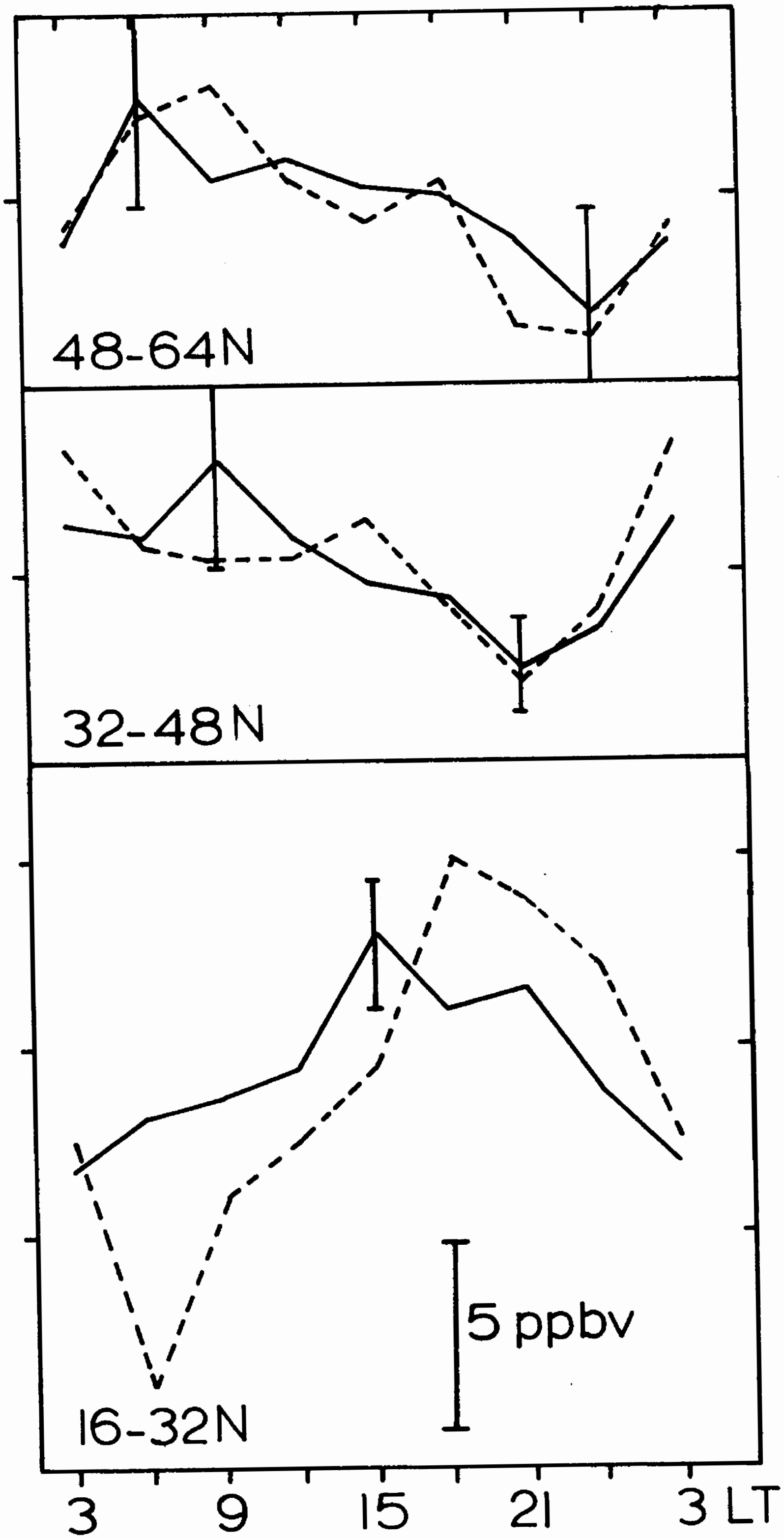

Figure 11. Annual mean deviations of trihourly ozone from seasonal means to show diurnal waveform in upper tropospheric ozone, by latitude; see text. The solid (dashed) line is for data from 50-70 hPa (30-50 hPa) below the tropopause. Estimates of one standard error are given for the solid lines at selected points. The vertical scale is illustrated in the bottom panel.

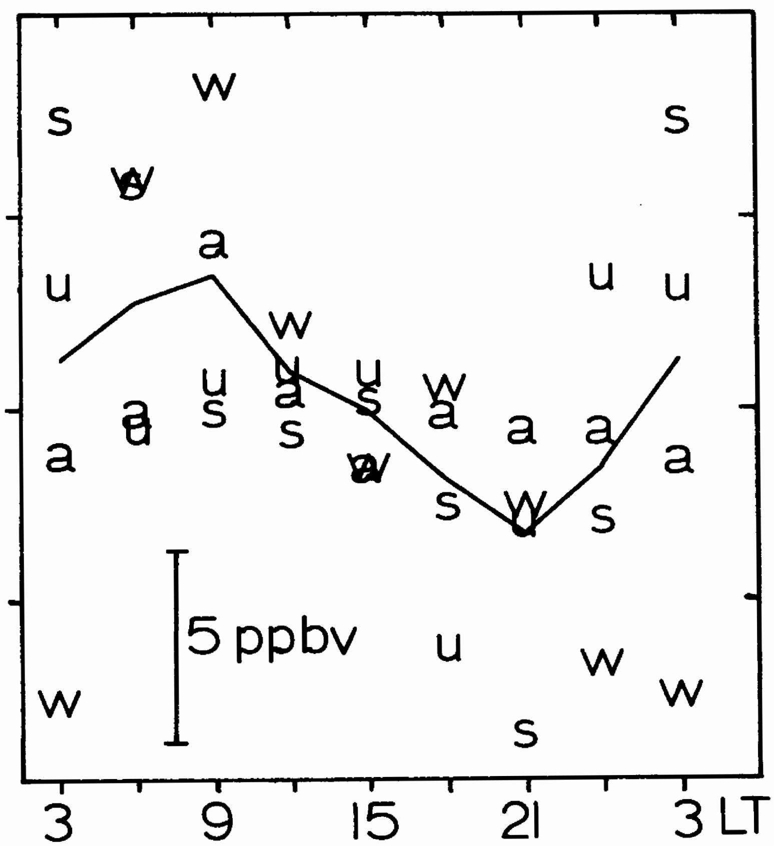

Figure 12. Mean deviation by season of trihourly ozone from seasonal means at 32-48N and 30-50 hPa below the tropopause. Similar to Figure 11 (center panel, dashed line) except that the annual mean (the solid line here) is the average of the four seasonal values without weighting by number of observations. Code: s = spring, u = summer a = autumn, w = winter.

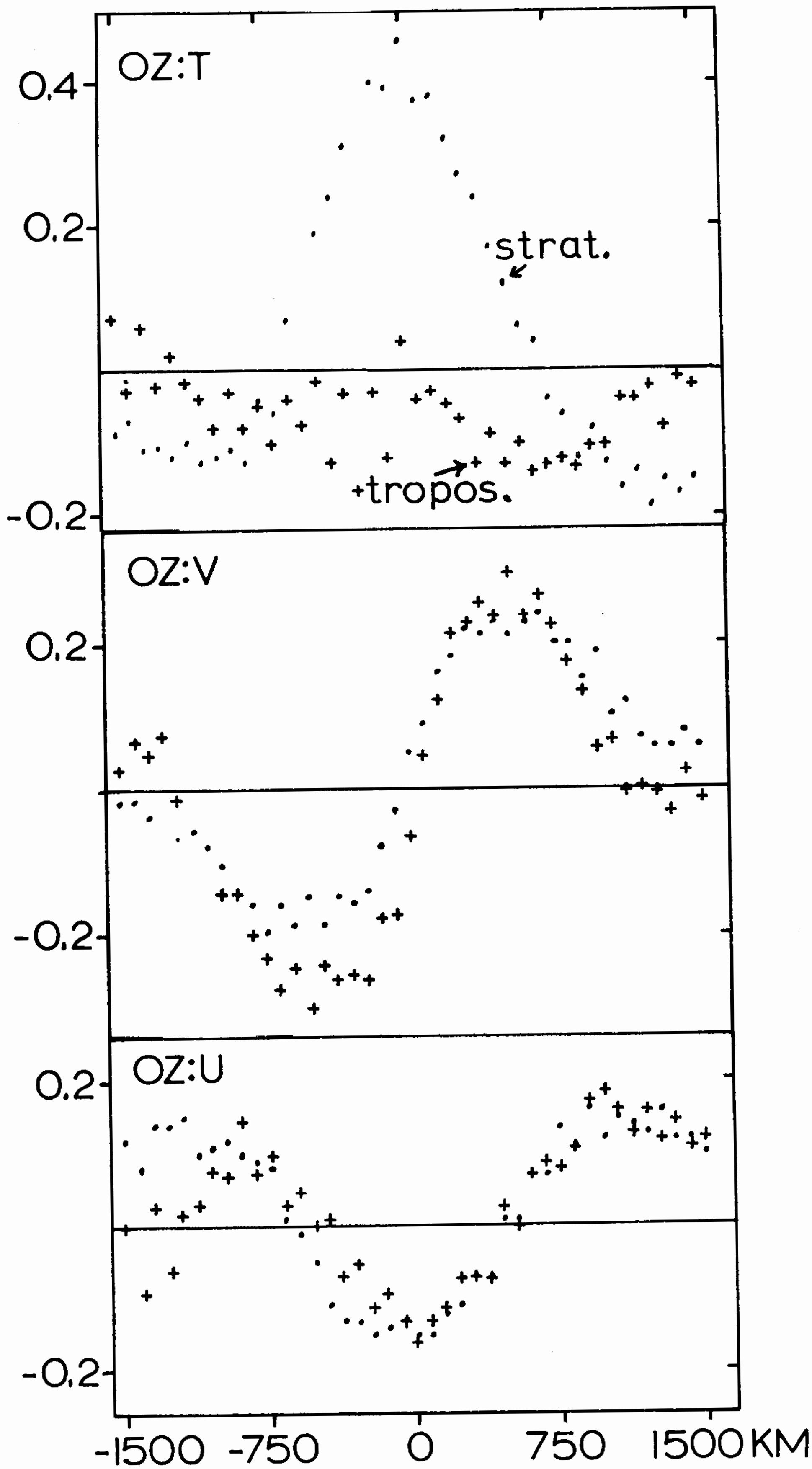

Figure 13. Distance-lagged cross-correlation function along selected E-W flight legs for ozone and (a) temperature, (b) meridional wind, (c) zonal wind. Dots are for stratospheric data and crosses for tropospheric data. See text.

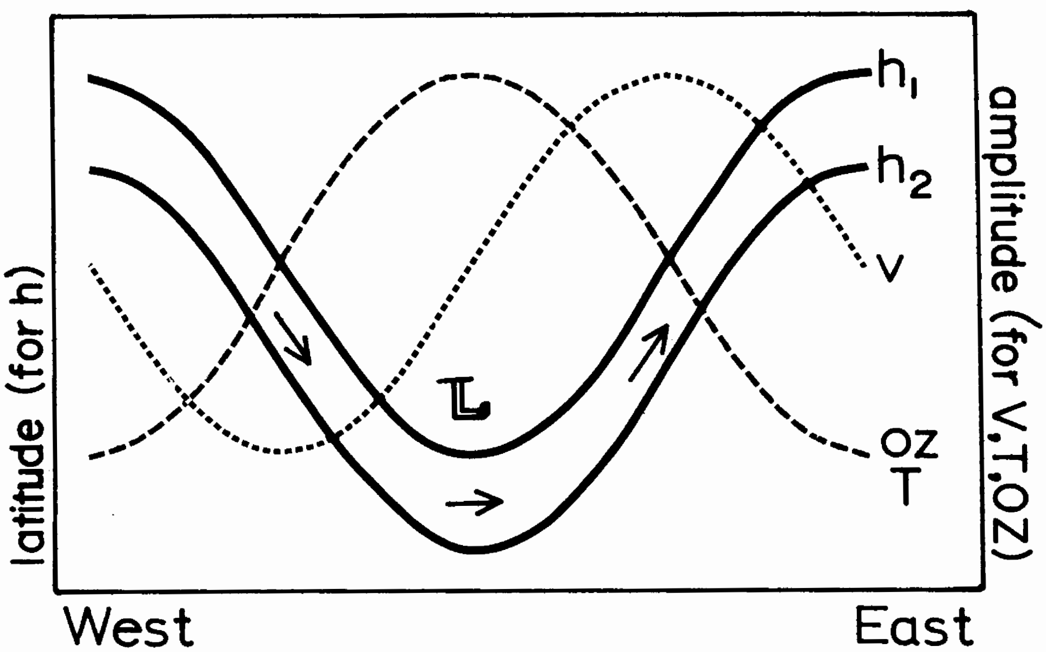

Figure 14. Schematic picture showing the phase relations between pressure-height, geostrophic meridional wind, and ozone and temperature. At a given pressure near the tropopause, largest ozone is found with lowest height.

APPENDIX A

GASP ozone data (ppbv) from 11 to 12 km true altitude as a function of latitude and longitude. The plotting code is in the upper left box. The right hand column is the zonal mean, and the max is the largest value at that latitude. The standard deviation (σ) is not given for fewer than ten observations.

120E 170E 140W 90W 40W 10E 60E 120E M

Mean N Max σ	484 9 584	483 30 937 154		540 9 598			493 48 937 127
	475 2 491	417 23 886 203	625 15 803 151	341 83 700 168			392 123 886 195
733 7 1169	472 22 1159 237	376 16 697 233	425 93 983 199	292 148 640 173	374 2 428		364 288 1169 213
288 16 777 209	293 60 669 180	420 199 994 233	347 157 808 192	140 26 517 138	411 31 801 172		361 489 994 218
184 41 596 153	332 32 635 184	290 641 964 221	222 36 825 217		294 4 464		283 754 964 218
131 33 324 74	109 76 265 45	127 421 582 100	126 21 580 140		229 29 538 165		130 580 582 102
84 40 142 26	92 372 378 41	89 84 143 33	61 13 96 19		130 1 130	81 66 159 29	89 576 378 38
52 48 96 20	77 265 293 46	39 43 255 45	51 7 60			52 66 112 29	66 429 293 43
40 143 104 18	92 30 138 23	45 40 108 29	36 81 93 22			21 41 59 16	42 335 138 27
			31 103 89 19			38 15 45 5	32 118 89 18
			19 50 46 12				19 50 46 12
			13 30 45 15				13 30 45 15
			24 19 45 14				24 19 45 14
			19 13 38 9				19 13 38 9
			6 1 6				6 1 6

APPENDIX A. March, April, May

LAT	120E–170E	170E–140W	140W–90W	90W–40W	40W–10E	10E–60E	60E–120E	M
–66	Mean N Max σ	314 13 374 37	313 17 359 28					314 30 374 33
66–60		280 69 499 104	356 9 405	231 13 343 97	291 63 397 83			285 15~~3~~4 499 95
60–54	341 2 344	219 31 479 133	288 22 463 132	152 60 437 117	179 95 360 106	127 7 179		188 217 479 122
54–48		302 19 393 89	125 65 409 106	99 106 344 67	175 7 195	171 22 336 64		134 219 409 99
48–42	34 7 48		115 239 549 97	86 8 221		80 45 194 38		107 299 549 90
42–36	32 9 59	79 24 189 41	71 281 393 67			53 121 125 17		66 435 393 57
36–30	51 3 83	55 223 174 28	73 99 514 103			40 29 69 8	39 50 98 16	56 404 514 56
30–24		52 136 191 29				41 1 41	33 36 65 9	48 173 191 27
24–18	18 2 24	20 29 36 6		30 3 39			27 56 53 10	25 90 53 9
18–12	16 6 19	18 55 29 5		31 7 44			25 53 65 13	22 121 65 10
12–6	15 5 18	17 52 27 6		23 4 24			24 24 46 10	19 85 46 8
6–0								
0–S 6		20 5 22						20 5 22
S 6–12		19 1 19						19 1 19
12–18								
18–24								
24–30	124 20 178 38						76 5 123	115 25 178 41
30–36								
36–42								

APPENDIX A. June, July, August

LAT	120E	170E	140W	90W	40W	10E	60E 120E	M
AT	Mean N Max σ	340 170 653 106	255 116 542 127					305 286 653 122
66		324 285 661 107	248 136 537 116	262 25 540 145	188 135 439 111			272 581 661 125
60	283 38 562 171	273 138 573 118	143 46 337 74	91 176 389 80	126 195 475 96			161 593 573 127
54	91 93 338 72	176 88 401 101	129 85 509 126	92 282 376 72	60 19 106 20			109 567 509 92
48	74 152 324 49	147 2 217	80 305 441 73	99 48 321 65		53 17 65 7		80 524 441 65
42	45 3 71	41 27 74 23	55 366 284 31	36 19 45 5		43 7 50		53 422 284 30
36		43 249 137 24	46 53 116 27	32 19 47 6			42 17 56 7	43 338 137 23
30		38 92 102 22	59 9 72	31 15 47 7			44 10 83 14	39 126 102 20
24		34 3 51	52 4 58	46 25 93 19			9 1 9	45 33 93 19
18		41 6 48		53 26 74 9				51 32 74 10
12		35 4 47		65 25 108 23				61 29 108 24
6				68 49 109 21				68 49 109 21
0				60 44 83 15				60 44 83 15
6		50 10 104 28		55 49 85 13				54 59 104 16
12		86 1 86		60 21 100 18				61 22 100 18
18								
24	130 5 174							130 5 174
30	196 6 235							196 6 235
36		231 2 255						231 2 255
42								

APPENDIX A. September, October, November

LAT	120E–170E	170E–140W	140W–90W	90W–40W	40W–10E	10E–60E	60E–120E	M
–N 66	Mean N Max σ	315 13 656 124	299 11 541 144					307 24 565 133
N 66–60		345 22 561 155	161 14 296 89		60 4 121			252 40 561 166
60–54				96 37 497 139	195 24 429 152			135 61 497 152
54–48			216 90 1028 195	266 54 1074 266	261 23 497 142			238 167 1074 216
48–42	190 9 282		145 445 604 111	182 51 690 133				149 505 690 113
42–36		41 30 209 37	88 394 519 76					85 424 519 75
36–30		55 282 373 41	81 87 235 46					61 369 373 44
30–24		48 132 129 29	52 26 108 24				93 4 264	50 162 264 33
24–18	3 40 26 5	31 57 84 18	32 3 35				21 3 24	20 103 84 19
18–12		31 31 54 11						31 31 54 11
12–6		27 48 45 8						27 48 45 8
6–0		31 62 57 10						31 62 57 10
0–S 6		29 59 54 11						29 59 54 11
S 6–12		38 65 99 21						38 65 99 21
12–18		55 30 145 31						55 30 145 31
18–24	109 3 116	100 25 175 48						101 28 175 46
24–30	211 27 345 93	148 17 283 61						187 44 345 88
30–36	213 6 279	174 13 318 70						186 19 318 68
36–42								

APPENDIX A. December, January, February